

# Variation of transport coefficients for average fission dynamics with temperature and shape

Shuhei Yamaji<sup>1</sup>, Fedor A.Ivanyuk<sup>2,3</sup> and Helmut Hofmann<sup>2</sup>

*1) Cyclotron Lab., Riken, Wako, Saitama, 351-01, Japan \**

*2) Physik-Department der Technischen Universität München, D-85747 Garching, Germany †*

*3) Institute for Nuclear Research of the Ukrainian Academy of Sciences, Kiev-28, Ukraine*

April 15, 1996

## Abstract

We study slow collective motion at finite thermal excitations on the basis of linear response theory applied to the locally harmonic approximation. The transport coefficients for average motion, friction  $\gamma$ , inertia  $M$  and the local stiffness  $C$  are computed along a fission path of  $^{224}\text{Th}$  within a quasi-static picture. The inverse relaxation time  $\beta = \gamma/M$  and the effective damping rate  $\eta = \gamma/(2\sqrt{M|C|})$  are found to increase with temperature, but do not change much with the collective variable. The values found for  $\eta$  and  $\beta$  as well as their behavior with temperature are in accord with experimental findings.

PACS: -05.60.+w, 21.60.Cs, 21.60.Ev, 24.10Pa, 24.75+i

KEYWORDS: collective motion, nuclear dissipation, linear response

## 1 Introduction

The nature of nuclear dissipation is not well understood yet. For isoscalar modes at finite excitations the best information available at present comes from fission experiments, when comparing the decay rate of fission with the ones for emission of light particles or gamma rays. Nowadays it seems not only possible to deduce numbers for the effective damping rate  $\eta$  [1], [2] but to gain information about its temperature dependence as well [3]. The authors of [3] find an  $\eta$  which increases markedly with  $T$ , at small to moderately large values of the temperature.

Such behavior is hard to understand for macroscopic models for which friction is either treated on the basis of two body viscosity or on the wall formula [4], [5]. In the first case friction should decrease with  $T$  like  $T^{-2}$ , in the second it would practically stay constant. Both results represent two contrasting pictures of the nuclear dynamics. The first one assumes collision dominance, and

---

\*yamajis@rikexp.riken.go.jp

†hhofmann@physik.tu-muenchen.de

is thus related in a sense to the nuclear compound model or its classical analog, the liquid drop model. The second picture would apply if, between two encounters or "collisions" with the wall, the nucleons are allowed to move freely inside the nuclear medium, as is suggested by the models of independent particles. In principle, the other two transport coefficients appearing in  $\eta$ , namely  $M$ ,  $C$  must be expected to change with temperature, too. But for the macroscopic models just mentioned this dependence will be weak. Therefore, the observed increase of  $\eta$  with  $T$  gives strong evidence for the necessity of having a microscopic theory. One possible formulation of the problem and its solution is based on a specific application of linear response theory. For a detailed description of the latter we may refer to [6] - [8] and [9]. In the present paper this theory will be applied to continue previous microscopic computations of friction  $\gamma$ , inertia  $M$  and local stiffness  $C$ , such as the ones of [6] and [8]. The emphasis will be put on their dependence both on temperature  $T$  as well as on the collective coordinate  $Q$ .

## 2 The linear response approach to collective motion

In this section we only want to briefly outline some basic theoretical features to have the most relevant formulas ready for explaining our computational analysis; we will follow largely [10], [8] and [9].

Similar to the deformed shell model we assume to have a Hamiltonian  $\hat{H}(\hat{x}_i, \hat{p}_i, Q)$  at our disposal which depends on deformation through the shape variable  $Q$ . For the sake of simplicity we just take one such degree of freedom, which later-on shall be used to parameterize motion along some given fission path. However, it does not suffice to restrict this  $\hat{H}(\hat{x}_i, \hat{p}_i, Q)$  to the deformed shell model, for which one would have (for  $A$  particles)

$$\hat{H}_{sm}(\hat{x}_i, \hat{p}_i, Q) = \sum_{l=1}^A \hat{h}(\hat{x}_l, \hat{p}_l, Q) \quad , \quad (2.1)$$

where  $\hat{h}(\hat{x}_l, \hat{p}_l, Q)$  stands for the dynamics of particle  $l$ . First of all, the expectation value of  $\hat{H}_{sm}(\hat{x}_i, \hat{p}_i, Q)$  does not represent the system's total energy. Secondly, as it stands this Hamiltonian would not account for effects of collisions. Following [11] the first deficiency is easily cured by adding to the operator part  $\hat{H}_{sm}(Q)$  a c-number term to get a  $\hat{H}_{rmf}(Q)$  as the representative for the (renormalized) mean field. This c-number term can be chosen in such a way that the static expectation value of  $\hat{H}_{rmf}(Q)$  (i.e. the one calculated for a time independent  $Q$ ) contains the renormalization terms of the Strutinsky method. (We choose the notation of [9] which slightly differs from [11], but the connection between both is readily established). The second issue can be taken care of by adding the effects of collisions when treating dynamical forces. In principle one might write

$$\hat{H}(\hat{x}_i, \hat{p}_i, Q) = \hat{H}_{rmf}(Q) + \hat{V}_{res}^{(2)}(\hat{x}_i, \hat{p}_i) \quad (2.2)$$

with the restriction of having the residual two body interaction  $\hat{V}_{res}^{(2)}(\hat{x}_i, \hat{p}_i)$  appear only in dynamical quantities like the response functions. How that can be done in practice will be explained below. Here we just like to mention that we want to assume this *incoherent* interaction  $\hat{V}_{res}^{(2)}(\hat{x}_i, \hat{p}_i)$  to be *independent* of the collective coordinate  $Q$ .

With these precautions taken into account we may say the average  $\langle \hat{H}(\hat{x}_i, \hat{p}_i, Q) \rangle$  to represent the total energy  $E_{tot}(t)$  of the system, now even in a dynamical sense. However, in case that the nucleus is *isolated* this energy must be a *constant of motion*. Hence the equation of motion for the

$Q(t)$  can be constructed from energy conservation applying Ehrenfest's theorem [12]. This is to say we may write:

$$0 = \frac{d}{dt}E_{tot} = \dot{Q} \left\langle \frac{\partial \hat{H}(\hat{x}_i, \hat{p}_i, Q)}{\partial Q} \right\rangle_t \equiv \dot{Q} \langle \hat{F}(\hat{x}_i, \hat{p}_i, Q) \rangle_t \quad (2.3)$$

The remaining task then is to express the average  $\langle \hat{F}(\hat{x}_i, \hat{p}_i, Q) \rangle_t$  as a functional of  $Q(t)$ . It is here where we shall exploit the benefits of linear response theory. The relevant operator  $\hat{F}(\hat{x}_i, \hat{p}_i, Q)$  is seen to be given by the derivative of the mean field with respect to  $Q$ ; it is of pure one body nature as the residual interaction  $\hat{V}_{res}^{(2)}(\hat{x}_i, \hat{p}_i)$  drops out when calculating this derivative.

## 2.1 Local linearization

Under certain circumstances, the task of evaluating the functional form of  $\langle \hat{F}(\hat{x}_i, \hat{p}_i, Q) \rangle_t$  can be simplified considerably. This will be so whenever the relevant  $Q$  can be handled as being close to some fixed value  $Q_0$ . Quite naturally this would be the case for harmonic vibrations about a stable potential minimum at  $Q_0$ . Fortunately, such a situation may be given even in the more general case. In this paper we restrict ourselves to study average dynamics, which means to neglect any statistical fluctuations in the variable  $Q$ , in which case it suffices to require collective motion to be sufficiently slow. Then  $Q$  will stay in the neighborhood of some properly chosen  $Q_0$  for some ("microscopically") large time interval  $\delta t$ ; if necessary one may interpret the  $Q_0$  as the  $Q(t)$  at a given time  $t_0$ .

For any  $Q$  close to  $Q_0$  one may evaluate the *intrinsic* quantity  $\langle \hat{F}(\hat{x}_i, \hat{p}_i, Q) \rangle_t$  by effectively using the Hamiltonian

$$\hat{H}(\hat{x}_i, \hat{p}_i, Q) = \hat{H}(\hat{x}_i, \hat{p}_i, Q_0) + (Q - Q_0)\hat{F}(\hat{x}_i, \hat{p}_i, Q_0) + \frac{1}{2}(Q - Q_0)^2 \left\langle \frac{\partial^2 \hat{H}}{\partial Q^2}(Q_0) \right\rangle_{Q_0, T_0}^{qs}, \quad (2.4)$$

instead of the original one. It is obtained by expanding to second order and by approximating the second order term within the unperturbed limit. The latter concept means to evaluate the expectation value on the very right by a *static* density operator which is given by  $\hat{H}(\hat{x}_i, \hat{p}_i, Q_0)$ . Effectively the only coupling term between collective and intrinsic motion is then given by the term of first order in  $Q - Q_0$ . It is not difficult to grasp the concept behind such an approximation: In this way global motion is described within a locally harmonic approximation. Here it was developed for average motion; a discussion of the general case can be found in [9]. One last remark on notation: In the sequel the  $\hat{F}(\hat{x}_i, \hat{p}_i, Q)$  shall be denoted by  $\hat{F}$  whenever it is to be taken at  $Q_0$ .

Applying the concept just described it can be shown (see e.g. [10] and [9]) that eq.(2.3) leads to the following form of the local equation of motion:

$$k^{-1}q(t) + \int_{-\infty}^{\infty} \tilde{\chi}(s)q(t-s)ds = 0. \quad (2.5)$$

Here  $q = Q - Q_m$  measures the deviation of the actual  $Q$  from the center of the oscillator approximating the true potential in the neighborhood of  $Q_0$ . The  $\tilde{\chi}$  is the causal response function associated to the dynamics of the nuclear "property"  $\langle \hat{F} \rangle$ . It is given by

$$\begin{aligned} \tilde{\chi}(t-s) &= \Theta(t-s) \frac{i}{\hbar} \text{tr}(\hat{\rho}_{qs}(Q_0, T_0) [\hat{F}^I(t), \hat{F}^I(s)]) \\ &\equiv 2i\Theta(t-s)\tilde{\chi}''(t-s) \end{aligned} \quad (2.6)$$

The expectation value appearing here is to be calculated like the one encountered in (2.4), namely by the density operator  $\hat{\rho}_{qs}$  which is determined by the Hamiltonian  $\hat{H}(Q_0)$  taken at  $Q_0$ . The same Hamiltonian is used to specify the time evolution in  $\hat{F}^I(t)$ . The  $\hat{\rho}_{qs}$  is meant to represent a thermal equilibrium at  $Q_0$  with excitation being parameterized either by temperature or by entropy. The quantity  $k$  summarizes contributions of static forces which appear in second order. Anticipating the change in entropy to be quadratic in  $\dot{q}(t)$ , one gets for the coupling constant  $k$ :

$$-k^{-1} = \langle \frac{\partial^2 \hat{H}}{\partial Q^2}(Q_0) \rangle_{Q_0, T_0}^{qs} + (\chi(0) - \chi^{ad}) \quad (2.7)$$

with  $\chi(0)$  being the static response (the Fourier transform of the time-dependent response function (2.6) taken at frequency  $\omega = 0$ ) and  $\chi^{ad}$  being the adiabatic susceptibility (sometimes  $\chi(0)$  is referred to as isolated susceptibility). It was shown in [10] that for temperatures not smaller than 1 to 1.5 MeV the coupling constant may effectively be calculated from the free energy  $f$ , or its stiffness  $\partial^2 f / \partial Q_0^2$ , rather, by the formula

$$-k^{-1} \simeq -k^{-1} \Big|_{T=const} = \frac{\partial^2 f}{\partial Q_0^2} \Big|_T + \chi(0) \quad (2.8)$$

## 2.2 Transport coefficients from the collective response

Transport coefficients parameterize properties of a system whose time development is described by differential equations. The easiest way of getting such an equation from the integral form (2.5) is to expand the factor  $q(t-s)$  under the integral to second order in  $s$  [12]. In this way the common equation of motion of the damped oscillator is obtained

$$M\ddot{q}(t) + \gamma\dot{q}(t) + Cq(t) = 0 \quad (2.9)$$

and the transport coefficients attain the forms:

$$M = M(0) = -\frac{1}{2} \int_{-\infty}^{\infty} \tilde{\chi}(s) s^2 ds = \frac{1}{2} \frac{\partial^2 \chi}{\partial \omega^2} \Big|_{\omega=0} \quad (2.10)$$

$$\gamma = \gamma(0) = \int_{-\infty}^{\infty} \tilde{\chi}(s) s ds = \frac{\partial \chi''}{\partial \omega} \Big|_{\omega=0}. \quad (2.11)$$

$$C = C(0) = -\chi(0) - k^{-1} = \frac{\partial^2 f}{\partial Q_0^2} \Big|_T \quad (2.12)$$

They follow after evaluating the moments in time of the response function through Fourier transformation. The last equality in eq.(2.12) is a consequence of the expression (2.8) for the coupling constant. For obvious reasons the notion "zero-frequency limit" has been coined to portray the coefficients (2.10- 2.12).

We may note that the procedure just applied is borrowed from models where the basic equations of motion are of integro-differential type, and where the reduction to differential form commonly is referred to as Markov approximation. It is only because of the self-consistency underlying the derivation sketched above that in (2.5) the common inertial terms are missing. As typically they are of order zero in the coupling they would make up differential terms from the start. Unfortunately, for the present case the method behind to (2.9- 2.12) does not always lead to a decent approximation

of (2.5). Let us mention just two problems. The most stringent one can be seen in the fact that the expression for inertia, which is nothing else but an extension of the cranking inertia to the case of damped motion at finite temperature [12], may become negative. Secondly, as both (2.5) as well as (2.9) are homogeneous the transport coefficients obtained this way are defined up to a common factor at best. To obtain all three coefficients, namely inertia  $M$ , friction  $\gamma$  and stiffness  $C$ , one needs an additional information.

Following general concepts, such an information can be obtained from a response function which parameterizes *collective* motion locally, and which thus will be denoted  $\chi_{coll}(\omega)$ . It can be derived by introducing a (hypothetical) external force  $\tilde{f}_{ext}(t)\hat{F}$  and by evaluating how the deviation of  $\langle \hat{F} \rangle_\omega$  from some properly chosen static value reacts to this external field in linear order:  $\delta \langle \hat{F} \rangle_\omega = -\chi_{coll}(\omega)f_{ext}(\omega)$ . As shown in [10] and [9] the  $\chi_{coll}(\omega)$  can be brought to the form

$$\chi_{coll}(\omega) = \frac{\chi(\omega)}{1 + k\chi(\omega)} \quad (2.13)$$

which is known to be standard for the case of zero temperature (see e.g. [13] and [11]). For finite excitations one needs an additional condition, namely that the motion is ergodic [14], in the sense of having adiabatic and isolated susceptibility equal to each other:  $\chi(0) = \chi^{ad}$ .

The dissipative part of  $\chi_{coll}(\omega)$  represents the distribution of strength over various possible local modes, which exhibit themselves as individual peaks. The corresponding "dispersion relation" or secular equation

$$\frac{1}{k} + \chi(\omega) = 0 \quad (2.14)$$

is easily recognized to come from the Fourier transform of (2.5). A solution of (2.14) leads to complex frequencies  $\omega_\nu$ , which actually come in pairs  $\omega_\nu^\pm = \pm\mathcal{E}_\nu - i\Gamma_\nu/2$ . Each pair may now be associated to the solutions of the secular equation of a damped oscillator like (2.9). Any full solution of (2.5) should contain information about all these frequencies. However, a reduction from the integral equation to the differential equation may now be performed by only picking one such pair. Since we aim at describing *slow* collective motion, it is natural to take the lowest ones, say  $\omega_1^\pm$ . In addition to the two parameters appearing there we have as additional information the strength of the corresponding poles which enables one to evaluate all three transport coefficients  $M, \gamma$  and  $C$ . In practice this can be done by replacing

$$\begin{aligned} (\chi_{coll}(\omega))^{-1} \delta \langle F \rangle_\omega &= -f_{ext}(\omega) \\ \Downarrow \\ (\chi_{osc}(\omega))^{-1} \delta \langle F \rangle_\omega &\equiv k^2(-M\omega^2 - \gamma i\omega + C)\delta \langle F \rangle_\omega = -f_{ext}(\omega), \end{aligned} \quad (2.15)$$

which is to say by approximating the response associated of the low frequency mode by that of a damped oscillator with modified transport coefficients. In practice the latter can be found by fitting the dissipative part of the oscillator response to the peak in the original strength distribution  $\chi''_{coll}(\omega)$ .

The appearance of the factor  $k^2$  has a simple mathematical reason. Evaluating the contribution to the collective response from the two poles chosen, the numerator of (2.13) has to be calculated at the poles' frequencies, which in the  $\chi_{coll}(\omega)$  leads to the factor  $\chi(\omega_\nu^\pm) = -1/k$ . It should be noted that by construction the oscillator response introduced here is the one for the quantity  $\langle F \rangle_t$ , while the transport coefficients shown are those for the "Q-mode", which also appear in (2.9). Indeed, the form (2.13) is valid if average motion in  $F$  is related to the one in  $Q$  by  $k \langle F \rangle_t = Q(t) - Q_0$ .

Therefore, the corresponding transport coefficients must be related to each other like  $\mathcal{T}^F = k^2 \mathcal{T}$ , where  $\mathcal{T}$  stands for  $M, \gamma, C$ .

The transport coefficients introduced in this way reflect the structure of the collective response (2.13). Since the latter accounts for self-consistency between collective and intrinsic motion<sup>1</sup> we will at times call these coefficients the self-consistent ones. It is possible to relate them to the zero-frequency limit. Suppose the lowest pair of frequencies  $\omega_1^\pm$  lies sufficiently close to  $\omega = 0$ . Then the  $\omega_1^\pm$  may be obtained by expanding in (2.14) the  $\chi(\omega)$  to second order in  $\omega$  around  $\omega = 0$ . The result is easily recognized as the secular equation to (2.9) with the transport coefficients being given by (2.10 - 2.12). In [7] some conditions have been derived for the zero-frequency limit to apply. This has been done for the case where the collective response function  $\chi_{coll}(\omega)$  is well simulated by the oscillator response function  $\chi_{osc}(\omega)$ , i.e. where the reduction (2.15) does not imply any further approximation. From the equations shown in [7] it is easy to see that the following relations hold true:

$$C = C(0) \left( 1 + \frac{C(0)}{\chi(0)} \right) \quad (2.16)$$

$$\gamma = \gamma(0) \left( 1 + \frac{C(0)}{\chi(0)} \right)^2 \quad (2.17)$$

$$M = \left( \frac{C}{C(0)} \right)^2 \left( M(0) + \frac{\gamma^2(0)}{\chi(0)} \right). \quad (2.18)$$

Once more, the transport coefficients of the left hand side are the ones obtained for the fit and those of the right hand side represent the zero frequency limit of the Lorentzian defined by the  $M, \gamma, C$ . Indeed, it is easily seen from (2.13) that this functional form implies the  $\chi(\omega)$  to be also of the type of an oscillator response function once the  $\chi_{coll}(\omega)$  on the left hand side is replaced by  $\chi_{osc}(\omega)$ .

Before we continue we would like to demonstrate that this concentration in a low frequency peak can be considered realistic for many examples, provided the temperature is not too small. In Fig.1 we show the strength function  $\chi''_{coll}(\omega)$  at the potential minimum and at the saddle point, which later on will be called point A and C, respectively, for temperatures  $T = 1, 2, 3 \text{ MeV}$ . (Details of the computation will be explained in the next section). Whereas at A the strength distribution reflects the typical behavior of stable modes, the one at C corresponds to unstable motion. For stable motion peaks are seen at higher frequencies, but the latter get washed out with increasing excitation. These features have been recognized and discussed before in [15] for quadrupole vibrations of  $^{208}\text{Pb}$ . The resulting concentration in a low frequency mode is even more clearly seen at the instability, where it occurs already at the smaller temperature of  $T = 1 \text{ MeV}$ . We should like to stress that this somewhat peculiar behavior of having the main peak in the strength distribution appear at very low frequencies is strongly related to the fact of the motion being overdamped. This feature can be made quantitative for the case of the oscillator response introduced in (2.15). It is easy to convince oneself that the position  $\omega_m$  of the maximum of  $\chi''_{osc}(\omega)$  is found at

$$\omega_m^2 = \frac{\varpi^2}{3} \left( 2\sqrt{1 - \text{sign}C\eta^2 + \eta^4} + \text{sign}C - 2\eta^2 \right) \quad (2.19)$$

where  $\varpi^2 = |C|/M$ . In the limit of  $\eta \rightarrow \infty$   $\omega_m$  turns to  $|C|/\gamma$  and the value of the response function taken at  $\omega_m$  is identical to  $\chi_{osc}(\omega_m) = 1/(2k^2|C|)$ .

---

<sup>1</sup>For instance, this feature may be deduced from the fact that for undamped motion (2.13) is identical to the response function of RPA, for the separable interaction  $(k/2)\hat{F}\hat{F}$ .

The procedure to obtain Eq.s.(2.16 to 2.18) may be turned around by starting with the coefficients of the zero frequency limit obtained from the original intrinsic response function. This implies to expand the  $(\chi_{coll}(\omega))^{-1} = k + (\chi(\omega))^{-1}$  to second order in  $\omega$  (with the  $\chi(\omega)$  being the full intrinsic response and not the one corresponding to the Lorentzian fit). In this way approximate versions of the self-consistent transport coefficients are obtained. It so turns out that they obey the same relation to the zero-frequency limit as given by (2.16 - 2.18). Later on we shall compare numerically the  $M, \gamma, C$  of (2.16 - 2.18) with the corresponding coefficients obtained by the fit indicated in (2.15). We may indicate already here that typically  $C(0)/\chi(0)$  is very small and decreases with temperature. This can be inferred from the fact that  $C(0)$  drops with increasing excitation whereas  $\chi(0)$  turns out quite insensitive to changes in  $T$  (c.f.[10]). For realistic cases, say above  $T \approx 1 MeV$ ,  $C(0)/\chi(0)$  is of the order of several %. For this reason the  $C$  and the  $\gamma$  of (2.16) and (2.17) get close to their zero-frequency value. It is only the inertia  $M$  of (2.18) which may differ considerably from  $M(0)$ , as a consequence of the second term in the second bracket. It is interesting to note, that at  $T = 0$  the ratio  $C(0)/\chi(0)$  might become of order unity if the spin-orbit interaction would not play a crucial role. This fact may be inferred from the analysis of quadrupole vibrations presented in sect.8.5 of [11] (from eq.(8.5.13b) it can be deduced that in this case  $C(0)/\chi(0)$  becomes identical to unity).

### 2.3 Collisional damping of nucleonic motion

Let us turn to the damping mechanism used in our theory. From the discussion of (2.2) one may anticipate that finally it is the residual two-body interaction  $V_{res}^{(2)}(\hat{x}_i, \hat{p}_i)$  which causes damping, first on the microscopic level, and then by way self-consistency for the collective motion as well. Because of the assumption of this interaction being independent of  $Q$  it enters the game only through the Hamiltonian  $\hat{H}(\hat{x}_i, \hat{p}_i, Q_0)$  which appears explicitly in the response function (2.6). To evaluate this expressions fully for some given  $V_{res}^{(2)}$  would be too a tremendous task. We therefore use a scheme which borrows from the way one would treat the effects of collisions in time dependent mean field theories like ETDHF or its classic versions as given by the BUU or Landau-Vlasov equation. In this paper we will just state the final expressions referring both to [9] as well as to earlier publications (for detailed lists see [6] and [8]).

The Fourier transform of the dissipative part of the intrinsic response function finally writes like

$$\chi''(\omega) = \int \frac{d\hbar\Omega}{4\pi} \left( n(\Omega - \frac{\omega}{2}) - n(\Omega + \frac{\omega}{2}) \right) \sum_{jk} |F_{jk}|^2 \varrho_k(\Omega - \frac{\omega}{2}) \varrho_j(\Omega + \frac{\omega}{2}) \quad (2.20)$$

Here,  $n(x)$  is the Fermi function determining the occupation of the single particle levels  $|k\rangle$ . The latter are the eigenstates of the Hamiltonian  $\hat{h}(\hat{\vec{x}}, \hat{\vec{p}}, Q_0)$  with corresponding energies  $\epsilon_k$ . The  $\varrho_k(\omega)$  represents the distribution of the single particle strength over more complicated states. It is here that the effects of collisions come into play. Neglecting them, which in our present language means to say putting  $V_{res}^{(2)}$  equal to zero, the  $\varrho_k(\omega)$  would simply be given by  $\varrho_k(\omega) = 2\pi\delta(\hbar\omega - \epsilon_k)$ . Conversely, a finite  $V_{res}^{(2)}$  gives reason for finite self-energies for which both real and imaginary parts are considered according to the formulae  $\Sigma(\omega, T) = \Sigma'(\omega, T) - i\Gamma(\omega, T)/2$ , with

$$\Gamma(\omega, T) = \frac{1}{\Gamma_0} \frac{(\hbar\omega - \mu)^2 + \pi^2 T^2}{1 + \frac{1}{c^2} [(\hbar\omega - \mu)^2 + \pi^2 T^2]} \quad (2.21)$$

and  $\mu$  being the chemical potential. Then the  $\varrho_k(\omega)$  becomes

$$\varrho_k(\omega) = \frac{\Gamma(\omega, T)}{(\hbar\omega - e_k - \Sigma'(\omega, T))^2 + \left(\frac{\Gamma(\omega, T)}{2}\right)^2} \quad (2.22)$$

In (2.21) the  $1/\Gamma_0$  represents the strength of the "collisions", viz the coupling to more complicated states. The cut-off parameter  $c$  allows one to account for the fact that the imaginary part of the self-energy does not increase indefinitely when the excitations get away from the Fermi surface. In the present calculation we choose  $\Gamma_0^{-1} = 0.03 MeV^{-1}$  and  $c = 20 MeV$ .

So far it was not specified whether or not the sum over  $j, k$  should include diagonal matrix elements. Quite generally, they measure quasi-static properties of the system and they are responsible for the "heat pole". The latter shows up at  $\omega = 0$  either in the relaxation function or in the correlation function associated to the dissipative part of the response. It was argued in [8] to neglect contributions from this heat pole, last not least to force ergodicity to be given. Within our model this implies to restrict the summation in eq.(2.20) to non-diagonal matrix elements. Such a restriction has thus been done also in the present computations. A more elaborate discussion will be published in [16].

## 2.4 Friction in zero-frequency limit

Because of its great importance we like to address specifically the calculation of the friction coefficient, in particular its temperature dependence. The origin of the latter can be made transparent for the zero-frequency limit. As we shall see below, numerical evidence tells one that this limit represents the actual value quite well for not too small temperatures (c.f. also [6], [7] and [16]). So let us evaluate  $\gamma(0)$  by inserting eq.(2.20) into eq.(2.11). One obtains:

$$\gamma(0) = - \int \frac{d\hbar\Omega}{4\pi} \frac{\partial n(\Omega)}{\partial \Omega} \sum_{jk} |F_{jk}|^2 \varrho_k(\Omega) \varrho_j(\Omega). \quad (2.23)$$

This expression can be simplified further using the Sommerfeld expansion for  $n(\Omega)$ . To leading order one gets [9]

$$\gamma(0) \approx \frac{\hbar}{4\pi} \sum_{jk} |F_{jk}|^2 \varrho_j(\mu) \varrho_k(\mu) \quad (2.24)$$

Here, the spectral density  $\varrho_k(\mu)$  is to be calculated at the frequency  $\hbar\omega = \mu$ . According to (2.21) this implies to use for  $\Gamma(\mu, T)$  a constant value, independent of  $\omega$ . For such a situation it does not make much sense to use refinements like the cut-off in the frequency dependence. Moreover, as the real part of the self-energy vanishes at  $\hbar\omega = \mu$  (see [9]) we may use

$$\Gamma(\mu, T) = \frac{1}{\Gamma_0} \pi^2 T^2 \approx 0.3 T^2 \quad (2.25)$$

and

$$\varrho_k(\mu) = \frac{\Gamma(\mu, T)}{(e_k - \mu)^2 + \frac{1}{4}\Gamma^2(\mu, T)} \quad (2.26)$$

It may be noted that this approximation is very much related to the typical relaxation time approximation to the collision term of the BUU or Landau-Vlasov equation, where commonly frequency



dependences of the relaxation time are also discarded (see [9]). Finally we may note that for the simple model outlined here the dependence of  $\gamma(0)$  on  $T$  appears to be synonymous that on the (constant) damping width  $\Gamma$ .

The validity of the Sommerfeld expansion has been studied numerically by computing eq.(2.23) for several temperatures (taking for  $\Gamma(\omega, T)$  a constant value  $\Gamma$ ). It was found that the temperature dependence due to  $n(\Omega)$  is weak, which in a sense justifies the use of (2.24). Therefore, a simple estimate of the temperature-dependence of friction may be obtained by using a constant width  $\Gamma$  and by relating the latter to  $T$  by way of (2.25).

In the case of no spin-orbit coupling, the explicit dependence of  $\gamma(0)$  on  $\Gamma$  may be simplified even more for the nucleus consisting of  $A/2$  protons and  $A/2$  neutrons, which occupy oscillator shells with principal quantum numbers  $1, 2, \dots, N$ . For quadrupole vibrations around a sphere one may use the same model as described in sect.8.5 of [11]. Applying this to (2.24) with (2.26) one gets

$$\gamma(0)/\hbar \approx \frac{4\Gamma^2(2\hbar\omega_0)^2\sigma}{9\pi[(\hbar\omega_0)^2 + \Gamma^2]} \left[ \frac{1}{(3\hbar\omega_0)^2 + \Gamma^2} + \frac{1}{(5\hbar\omega_0)^2 + \Gamma^2} + \dots \right] \quad (2.27)$$

The quantity  $\sigma$  represents the dependence of the average squared matrix elements on  $N$ . To leading order one gets  $\sigma \simeq (\frac{3}{2}A)^{\frac{4}{3}}$  (c.f.[11]).

## 2.5 The single-particle Hamiltonian

For the present computation the single particle Hamiltonian  $\hat{h}(\hat{x}, \hat{p}, Q)$  of (2.1) is chosen to be given by the two-center shell model of [17] and [18]:

$$\hat{h} = -\frac{\hbar^2 \nabla^2}{2m} + \hat{V}(\hat{\rho}, \hat{z}) + \hat{V}_{ls}(\hat{x}, \hat{l}, \hat{s}) + \hat{V}_{l^2}(\hat{x}, \hat{l}) \quad (2.28)$$

Here  $V$  is the two-center potential in cylindrical coordinates with  $m$ ,  $\hat{s}$  and  $\hat{l}$  being the nucleons' mass and the operators for spin and angular momentum, respectively. A detailed description of the construction of  $V$  can be found in [17]; the version of [18] is more general. As basic shape parameters there are the distance  $z_0 = z_2 - z_1$  between the centers  $z_i$  of the two potential wells, a neck-parameter  $\epsilon$  and a mass ratio  $\alpha$ ; whereas in [17] the two fragments where of spherical shape, in [18] finite deformations  $\delta_1, \delta_2$  are introduced. To demonstrate the geometrical meaning of the shape variables, we show in Fig.2 the potential along the z-axis and the associated nuclear shape. As usual the nuclear surface is identified as an equipotential one of the two-center potential, and volume conservation is required for the uniform density inside the surface corresponding to the Fermi energy. The volume then has a value given by the sphere with radius  $R_0 = r_0 A^{1/3}$ , with  $A$  being a mass number of the nucleus. In the present calculation, we take the radius parameter  $r_0$  to be equal to 1.2 fm. The associated oscillator frequency  $\hbar\omega_0$  for the spherical shape is then given by  $\hbar\omega_0 = 41A^{-1/3}$ .

The momentum-dependent part in eq.(2.28) consist of a spin orbit-coupling term  $\hat{V}_{ls}$  and an  $l^2$ -term  $\hat{V}_{l^2}$ . For them the angular momentum  $\hat{l}$  is described in the stretched coordinates. The strengths  $\kappa_i$  of  $ls$ - and  $\kappa_i\mu_i$  of  $l^2$ - are taken from [19]. For a given shape the Hamiltonian (2.28) is diagonalized within the basis of eigen-functions constructed for the the two-center potential without a "neck-correction term"; hereto states up to energies of  $(N_0 + 3/2)\hbar\omega_0$  are taken into account, with  $N_0 = 20$ . The "neck-correction term" is used to remove the cusp which naturally arises at  $z = 0$  if one just puts together two oscillator potentials (see Fig.2; for more details we refer to [17] [18]).

The deformations  $\delta_i$  of the fragments are described by the ratio of the semi-axes  $a_i$  and  $b_i$  as  $a_i/b_i = \sqrt{(1 + 2/3\delta_i)}/\sqrt{(1 - 4/3\delta_i)}$ , with  $i = 1$  and  $2$  for the left and right fragments. The neck-parameter  $\epsilon$  is defined as the ratio  $\epsilon = V_0/V'$  with  $V_0$  and  $V'$  being the heights of the potential barrier at the origin, calculated with and without the "neck-correction term", respectively.

As mentioned earlier the transport coefficients shall be computed along a "fission path" only. In this paper we want to identify the latter with a line of minimal potential energy. This energy shall be approximated by the one of the cold liquid drop, calculated for a two dimensional subspace, which comes about in the following way: We concentrate on symmetric fission, for which the mass ratio  $\alpha$  becomes unity, and choose the deformations of the left and right fragments to be equal to each other, which means to have  $\delta_1 = \delta_2 = \delta$ . Finally, the neck parameter, which is sensitive to specifications of the scission configuration, is fixed to the value  $\epsilon = 0.4$ . In a previous study [20] this value has been seen to reproduce well the observed average kinetic energy for thermal fission of  $^{200}\text{Pb}$ . The family of shapes from which the "fission path" is evaluated is defined by the two parameters  $z_0$  and  $\delta$ , and the motion along it shall be parameterized by a variable  $r_{12}$ . It is defined as the ratio  $r_{12} = R_{12}/(2R_0)$ , where  $R_{12} = R_2 - R_1$  measures the relative distance between the centers of mass of the two fragments (see Fig.2), and  $R_0$  stands for the radius of the spherical configuration. For this variable  $r_{12}$  the single-particle operator  $\hat{F}$  is defined as

$$\hat{F} = \frac{\partial \hat{h}}{\partial r_{12}} = \left( \frac{\partial r_{12}}{\partial z_0} + \frac{\partial \delta}{\partial z_0} \frac{\partial r_{12}}{\partial \delta} \right)^{-1} \left( \frac{\partial \hat{h}}{\partial z_0} + \frac{\partial \delta}{\partial z_0} \frac{\partial \hat{h}}{\partial \delta} \right) \quad (2.29)$$

where the derivative  $\partial \delta / \partial z_0$  is to be taken along the fission path  $\delta = \delta(z_0)$ .

## 2.6 The deformation energy

For the collective response function eq.(2.13), we need the coupling constant  $k$  as given by eq.(2.8). This expression can be evaluated from the free energy  $f$  and the static response  $\chi(0)$ . The free energy  $f(r_{12}, T)$  will be written as a sum of Coulomb and surface energies plus the shell correction part:

$$f(r_{12}, T) = f_{Coul}(r_{12}, T) + f_{surf}(r_{12}, T) + f_{sc}(r_{12}, T). \quad (2.30)$$

The free Coulomb and surface energies is approximated by

$$f_{Coul}(r_{12}, T) = f_{Coul}(r_{12}, T = 0)(1 - \alpha T^2) \quad (2.31)$$

and

$$f_{surf}(r_{12}, T) = f_{surf}(r_{12}, T = 0)(1 - \beta T^2) \quad (2.32)$$

with the values of  $\alpha$  and  $\beta$  taken to be 0.000763 and 0.00553  $\text{MeV}^{-2}$  [21]. The free energies  $f_{Coul}(r_{12}, T = 0)$  and  $f_{surf}(r_{12}, T = 0)$  have been evaluated according to [22]. In Table III of [22], there are several sets of parameters. Here, we choose the set with the values of  $a = 0.65 \text{ fm}$ ,  $a_s = 21.836 \text{ MeV}$ ,  $K_s = 3.48$  corresponding to the radius parameter  $r_0 = 1.2 \text{ fm}$ . For the shell correction we assume the form (c.f.[13]):

$$f_{sc}(r_{12}, T) = f_{sc}(r_{12}, T = 0)\tau / \sinh \tau \quad (2.33)$$

with  $\tau = (2\pi^2 T)/(\hbar\omega_0)$ . The shell correction  $f_{sc}(r_{12}, T = 0)$  is evaluated according to [23].

### 3 Numerical results

We want to evaluate transport coefficients along the fission path for symmetric fission of  $^{224}\text{Th}$  and like to study their dependence on temperature  $T$  and their variation with the shape variable. As previously mentioned, the fission path will be defined through the static energy.

#### 3.1 The static energy and the stiffness coefficient

In Fig.3 the liquid-drop energy  $V_{LDM}(z_0, \delta) = f_{Coul}(T = 0) + f_{surf}(T = 0)$  is shown as function of  $z_0$  and  $\delta$ . The curve along which this energy is minimal for each  $z_0$  is given by the long-dashed curve. It connects the point A of the spherical shape with the saddle point C and then follows down to the scission configuration. The latter part reflects the path of steepest decent. This trajectory is taken as our "the fission path". It is clear that such a static path will have to change with temperature, because of the dependence on  $T$  of both the shell correction as well as of the macroscopic free energy. Such refinements are neglected here.

In Fig.4, we plot the free energy  $f(r_{12}, T)$  as a function of the shape variable  $r_{12}$  for different values of  $T$  along the fission path shown in Fig.3. We restrict ourselves to  $T \geq 1\text{MeV}$  and neglect pairing correlations, which should be taken into account for quantitative studies at lower temperatures. The second derivative of the free energy  $C(0) = \partial^2 f / \partial Q_0^2$  is plotted in Fig.5 as function of  $T$ . At not too small temperatures the actual stiffness  $C$  turns out to be close to this zero-frequency limit; (2.16) and the discussion given there.

#### 3.2 The friction coefficient

##### a) A schematic study of the zero frequency limit

We first would like to work out a few general features at the example of the zero-frequency limit (2.24) applied to quadrupole vibrations. In Fig.6 the result of a computation is shown for the doubly closed shell nuclei  $^{140}\text{Yb}$  and  $^{208}\text{Pb}$ , neglecting spin-orbit coupling in the first case. For the width the formula  $\Gamma(\mu, T) = 0.3T^2$  is used and as single particle model a harmonic oscillator is taken with spheroidal deformation  $\delta$ . For small deformations this  $\delta$  is related to  $\alpha_2$  by  $\delta \sim (15/8\pi)\alpha_2$ , where  $\alpha_2$  is the common parameter appearing in  $(R = R_0(1 + \alpha_2 Y_{20}(\theta, \varphi)))$  [13], [11].

Fig.6 shows that at small  $T$  friction increases strongly with  $T$ , then it reaches some maximal value at some  $T_{max}$  and decreases afterwards. Taken simply as function of the width  $\Gamma$ , such behavior may be inferred from the semi-analytical formula (2.27). With respect to the dependence on temperature one must be a little careful, as the result shown in the figure was obtained for  $\Gamma(\mu, T) = 0.3T^2$ , neglecting the influence of the cut-off parameter  $c$  in (2.21). A finite cut-off parameter would weaken the  $T$ -dependence somewhat (see [8]), but it should be clear that the present model study only aims at a qualitative understanding. After all we are neglecting subtle, but important details of collisional damping like the width's dependence on frequency. The value of the width  $\Gamma_{max}$  at which  $\gamma(0)$  reaches its maximal value is strongly related to the energy differences  $|e_j - e_k|$  of those single-particle pairs  $(j, k)$  which give significant values to the transition matrix element  $|F_{jk}|^2$ . From eq.(2.27) one may deduce this  $\Gamma_{max}$  to be of the order of  $\hbar\omega_0$  in case of no spin-orbit coupling. With spin-orbit coupling the values of  $\Gamma_{max}$  will get smaller, since then there will be important contributions from pairs  $(j, k)$  which lie closer in energy. The corresponding  $T_{max}$  may be estimated to  $0.3 \times T_{max}^2 \approx \Gamma_{max}$ . For example, it can be seen that the values of  $T_{max}$  are 6.7 MeV for  $^{140}\text{Yb}$  and 2.5 MeV for  $^{208}\text{Pb}$ .

Let us address now the value of the friction coefficient and compare it with the wall formula. The maximal values of  $\gamma(0)/\hbar$  are seen to be 40 and 180 for  $^{140}\text{Yb}$  and  $^{208}\text{Pb}$ , respectively. These numbers reflect a general behaviour in that friction can be said to become larger if the spin-orbit coupling is taken into account, for given mass number. However, altogether the magnitude is much smaller than that of the wall formula, for which one would get 530 and 900 for the two cases considered, namely  $^{140}\text{Yb}$  and  $^{208}\text{Pb}$ , respectively. The latter numbers can be estimated as follows. For the spheroidal deformation  $\delta$  the wall friction [4]

$$\gamma_w = \frac{3}{4} \rho v_F \oint v_n^2 dS \quad (3.1)$$

can be shown to reduce to the simple expression  $\gamma_w/\hbar = \frac{2\pi}{25} \sqrt[3]{9\pi} A^{\frac{4}{3}} \approx 0.76 A^{\frac{4}{3}}$  ( $\rho$  is the particles density,  $v_F$  - Fermi velocity,  $v_n$  - wall velocity normal to surface).

The small value obtained for our friction coefficient is related to the "gap" in the single-particle spectrum, which in the expressions for the friction coefficient appears in the denominators (mind (2.27)). For doubly closed nuclei the contribution to friction comes from states whose energy difference  $|e_j - e_k|$  is rather large. This energy difference becomes especially large for the spherical oscillator potential (for which only states with  $|e_j - e_k| = 2\hbar\omega_0$  contributes to response function and consequently to the friction).

## b) General results

Let us turn now to discuss results which are obtained using our complete theoretical input, namely the realistic two center shell model, applied to expression (2.20), with the collisional damping as given by (2.22) and (2.21), together with the realistic coupling constant. The coefficient  $\gamma$  is shown in Fig.7 as function of temperature, for the points A and C along the fission path indicated in Fig.3. For comparison on the right the values of the so called modified wall formula are shown as well, which reads  $\gamma_{m.w} = 0.27\gamma_w$  [24].

Two computations are presented, one based on the fit of the oscillator response (see (2.15) and one based on the formula (2.17) (with  $C(0)$ ,  $\chi(0)$  and  $\gamma(0)$  being calculated from the original  $\chi(\omega)$ , without employing any fit). It is seen that both results agree almost perfectly well for all temperatures used at those points where the local stiffness is negative, and where, hence, the local motion is unstable. At the stable point A there is some disagreement at smaller temperatures, but even at  $T = 1 \text{ MeV}$  the difference is smaller than about 30% and at  $T = 1.5 \text{ MeV}$  it is almost negligible. The origin of the deviation of these two computations from each other can easily be understood looking at the collective strength distributions discussed above with the help of Fig.1. It is only for small temperatures that this distribution cannot be approximated by one Lorentzian. We should like to note that the friction coefficient given by (2.17) is almost identical to the one of the zero-frequency limit. The correction given by  $(C(0)/\chi(0))^2$  only amounts to about 4%.

Finally, we exhibit in Fig.8 the coordinate dependence of the friction coefficient for various temperatures. It so turns out that for the present case the result at  $T = 1 \text{ MeV}$  is very well represented by the modified wall formula.

## 3.3 Mass parameter

Finally we turn to the inertia for which some new problems appear, as may be demonstrated with the help of Fig.9. There the temperature dependence is exhibited for three computations of the inertia, performed at the point A. Firstly, there is the one from the fit and secondly the one

calculated from the expression (2.18). Like for the case of friction, both agree with each other for higher temperatures, say above  $1.5 \text{ MeV}$ , and for the same reason. Above this temperature there essentially no higher modes exist, at least for the present model. It is important to note that now, different to the case of friction, the zero-frequency limit  $M(0)$ , as given by the "cranking inertia" (2.10) fails to be a reasonable approximation. Looking at (2.18) it is only by way of the second term in the second bracket that the  $M$  calculated this way is close to the one of the fit. As has been noted before, the zero-frequency mass may get very small, often even negative.

Let us address now the third curve of Fig.9, which is marked by "sum rule". As is well known from the case of zero damping, see e.g. [13] or [11], there should exist the following, general relation of the energy weighted sum to the inertias of the various possible modes with frequencies  $\omega_\nu^\pm$  (see also [9]):

$$\begin{aligned} S &= \langle [\hat{F}, [\hat{H}, \hat{F}]] \rangle = \frac{\hbar^2}{\pi} \int_{-\infty}^{\infty} d\omega \chi''_{coll}(\omega) \omega \\ &= \sum_{\nu} \frac{\hbar^2}{\pi} \int_{-\infty}^{\infty} d\omega \chi''_{osc}^{(\nu)}(\omega) \omega = \sum_{\nu} \frac{\hbar^2}{k^2 M(\omega_{\nu})} \end{aligned} \quad (3.2)$$

(Here, in the last expression again the factor  $k^2$  appears because we take the inertia's of the  $Q$ -mode, but related them to the sum of the  $F$ -modes). As may be inferred easily from this formula, the inertia of one mode cannot be smaller than  $\hbar^2/(Sk^2)$ . Unfortunately, this is not necessarily the case without further precautions.

Essentially two problems appear here. First of all, evaluating the integral

$$S = 2 \frac{\hbar^2}{\pi} \int_0^{\omega_{max}} d\omega \chi''_{coll}(\omega) \omega \quad (3.3)$$

as function of the upper limit  $\omega_{max}$  one realizes bad convergence. This fact is related to the construction of the response function, particularly that of  $\chi''$ . The forms given in (2.22) and (2.21) cannot be expected to be good at large frequencies. The second problem comes up whenever the single particle potential does not warrant the density of the shell model to agree sufficiently well with the one which is used in the definition of the shape variable. Usually, this is alright for the simple model of the deformed oscillator, for which it is easy to prove that the inertia corresponding to the total sum, i.e.  $\hbar^2/(Sk^2)$ , is given by the  $M_{irrot}$  irrotational flow. Indeed, for this case it has been possible in [15] to show that the self-consistent inertia  $M(\omega_1)$  turns into  $M_{irrot}$  for large temperatures. Again, the very fact that  $M(\omega_1)$  must approach the value given by the sum rule follows from the observation that with increasing excitation the strength concentrates in the low frequency mode.

In a forthcoming paper [16] we will try to solve the second problem mentioned above, which involves the relation of the density distribution to the shape of the potential. For the present case we suggest the following pragmatic procedure. We just fix the sum rule value by the inertia  $M_{irrot}$  of irrotational flow, which in turn is evaluated by the method of Werner-Wheeler [25]. To put it differently, we scale the inertia  $M = M(\omega_1)$  for the low frequency mode such that it becomes equal to  $M_{irrot}$  at large  $T$ . At smaller temperatures this  $M$  will attain larger values, of course. The result of such a computation is shown by that curve which in Fig.9 is marked by "sum rule".

In this context it is worth recalling that at somewhat larger temperatures collective motion gets overdamped such that inertia does not play a big role anymore. It is reassuring therefore to see that for such cases the fit of the oscillator response does not depend very much on the inertia (mind the discussion given above next to (2.19)).

In Fig.10 we address the coordinate dependence of the inertia, as obtained for various temperatures. From this figure one may observe that above  $T = 2 \text{ MeV}$  the values do not change anymore with excitation.

### 3.4 The inverse relaxation time $\beta = \gamma/M$

In the literature the quantity  $\beta = \gamma/M$  has come into use (see e.g.[1] to [3]) for parameterizing the strength of the friction force, where for  $M$  commonly the irrotational flow value is taken. The inverse quantity  $\beta^{-1}$  has a dimension of time and actually measures physically the (local) relaxation time to the Maxwell distribution in collective phase space. Taking our results for friction and inertia from Figs.8 and 10 we get a coordinate dependence of  $\beta$  as shown in Fig.11. It is seen that this dependence is much weaker than the one of  $\gamma$  and  $M$  themselves. This is to be expected in a sense, as any geometrical factor contained in the individual quantities drops out when building the ratio. Actually, the variation along the fission path is weaker than the one with excitation. Incidentally, it is seen that  $\beta$  decreases somewhat with deformation.

The values of  $\beta$  seen in Fig.11 are in the range of those published earlier for quadrupole vibrations of  $^{208}\text{Pb}$  [15] [8], having the tendency of being slightly smaller than in this previous case, which is no surprise in the light of the discussion presented above for friction. In any case, these values are comparable to those associated with "linear response theory" in the compilation given in Fig.13 of [2]. As seen from Fig.12 of the same paper, they are in reassuring agreement with numbers found adequate in many theoretical descriptions of fission accompanied by emission of light particles.

In Fig.11 our results for  $\beta$  are compared with that suggested by Fröbrich and Gontchar for a phenomenological description of fission of the type just mentioned [26]. Their deformation parameter  $q$  is the same as our parameter  $r_{12}$ . It may be said that their model has also been quite successful in explaining observed experimental data, but quite apparently, their  $\beta(q)$  is in violent contradiction to our picture. In case it will turn out that their model is safe otherwise, leaving no room for modifying the  $\beta(q)$ , one might be inclined to conclude that the friction necessary in this case must be of different physical origin. One possible candidate would be a dissipation mechanism which comes from the so called "heat pole" and which in [8] has been seen to be identical to the one of "adiabatic" motion [27]. This would be an interesting perspective as it might indicate that motion beyond the saddle is "fast", even at high excitations, in contradiction to the general believe.

### 3.5 The effective damping rate $\eta = \gamma/(2\sqrt{M|C|})$ and the dynamics of fission

For a damped oscillator the quantity  $\eta = \gamma/2\sqrt{M|C|}$  indicates whether motion is underdamped ( $\eta < 1$ ) or overdamped ( $\eta > 1$ ). Therefore, it is a good measure for the effective degree of damping, except around points of inflection where the local stiffness becomes zero. Furthermore, it is exactly this quantity, if calculated at the saddle point, which according to Kramers' famous formula

$$R_K = \left( \sqrt{1 + \eta_s} - \eta_s \right) \frac{\varpi_m}{2\pi} e^{-B/T} \approx \left( \sqrt{1 + \eta_s} - \eta_s \right) R_{BW} \quad (3.4)$$

determines the deviation of the fission decay rate  $R_K$  from the  $R_{BW}$  of the Bohr-Wheeler formula ( $\varpi^2 = |C|/M$ ). Within the linear response approach  $\eta$  has been calculated as function of  $T$  before (see [8]), but only for the case of quadrupole vibrations around the spherical minimum of lead. From all the information presented above we are now in the position of calculating  $\eta$  along the

fission path. However, in the light of formula (3.4) it may suffice first to study it around the barrier. Indeed, this formula applies if, from the full dynamics across the barrier, it is only the motion around the stationary points which matters. The latter situation can be seen to be given if the height  $B$  of the barrier is much larger than temperature:  $B/T \gg 1$  ([28], see also [29]). Effectively, one may then approximate the true barrier by a model potential which consists of one ordinary oscillator for the minimum plus an inverted one for the barrier, joined smoothly to each other (see [29]). Unfortunately, often (3.4) is applied even in cases that this basic condition on  $T$  and  $B$  is violated.

To study these questions for our example we have calculated all relevant quantities by performing averages both around the potential minimum as well as around the barrier. For the first case this means to average in the regime from  $r_{12} = 0.375$  to some value  $r_{12}^{(1)}$ , and for the second one from this  $r_{12}^{(1)}$  to some  $r_{12}^{(2)}$  behind the barrier. Both values depend on temperature, of course, as may be inferred from Fig.4. We took the values  $r_{12}^{(1)} = 0.47, 0.46, 0.45, 0.44, 0.42$  and  $r_{12}^{(2)} = 1.05, 0.96, 0.87, 0.74, 0.60$  for  $T = 1, 2, 3, 4, 5$  MeV, respectively. The results are put together in the following Table:

| $T$ | $C_m$ | $\hbar\varpi_m$ | $\beta_m$    | $\eta_m$ | $-C_s$ | $B$  | $\hbar\varpi_s$ | $\beta_s$    | $\eta_s$ |
|-----|-------|-----------------|--------------|----------|--------|------|-----------------|--------------|----------|
| MeV | MeV   | MeV             | MeV/ $\hbar$ |          | MeV    | MeV  | MeV             | MeV/ $\hbar$ |          |
| 1   | 538   | 0.82            | 1.8          | 1.1      | 109    | 7.20 | 0.50            | 1.2          | 1.2      |
| 2   | 509   | 0.94            | 4.2          | 2.2      | 131    | 5.95 | 0.59            | 3.2          | 2.7      |
| 3   | 472   | 0.93            | 4.8          | 2.5      | 134    | 4.31 | 0.59            | 3.8          | 3.2      |
| 4   | 407   | 0.87            | 4.6          | 2.7      | 152    | 2.59 | 0.60            | 4.0          | 3.3      |
| 5   | 335   | 0.79            | 4.6          | 2.9      | 200    | 1.18 | 0.67            | 4.1          | 3.0      |

Several inferences can be drawn immediately:

- In the values of  $\eta$  and  $\beta$ , as well as in their variation with  $T$  there is not much difference between the barrier and the minimum.
- The basic condition on the validity of (3.4) is satisfied for temperatures up to 3 MeV at best.
- It is interesting to note that  $\hbar\varpi_s$  increases with  $T$ , albeit only slightly.

A closer inspection shows the quantity  $2\pi T/(\hbar\varpi_s)$  to be of order  $\pi$  and thus definitely larger than unity. This implies that collective quantum effects do not contribute to fission dynamics for the examples chosen here. According to [29] for  $2\pi T/(\hbar\varpi_s) \ll 1$  such effects would change (3.4) to  $R = f_Q R_K$ , but quite apparently the quantum correction factor  $f_Q$  plays a role only at temperatures smaller than 1 MeV.

## 4 Summary, conclusion and outlook

In the previous sections we have presented a detailed microscopic study of transport coefficients for fission. They have been deduced within the quasi-static picture in which linear response theory is applied to describe motion around local thermal equilibrium. Following earlier work, the contribution from the "heat pole" to the response functions has been neglected. As described in [8], such a restriction is closely related to what in the context of nuclear physics one commonly associates with the "adiabatic" picture, in contrast to the "diabatic" one one would expect to apply for "fast" motion.

The response functions have been calculated within a realistic two-center shell model. Effects of collisions have been accounted for by using self-energies having both real and imaginary parts. The latter are allowed to depend not only on temperature but on frequency as well, in which way memory

effects of the collision term are simulated. Locally collective motion is treated self-consistently, in the sense that the structure of the associated response resembles the one known from the RPA of undamped motion.

Various procedures have been described to deduce transport coefficients from the microscopically computed response, which generalize previous descriptions. They have been evaluated as function both of temperature as well as of the variation of the shape along the fission path. Considering all the effects taken into account, such a study has never been reported before. The results found invite us to draw the following conclusions.

- Perhaps one of the most striking features is the weak dependence of both  $\beta$  as well as of  $\eta$  on the shape parameter, as encountered here along the fission path.
- The temperature dependence of these two quantities is similar to the one reported previously in [8] for vibrations of  $^{208}\text{Pb}$ : they increase with  $T$ , to eventually reach some saturation around  $T \approx 4 \text{ MeV}$ .
- This behavior is in agreement with findings reported in [3], at least qualitatively. Our damping rate is somewhat smaller, and its variation with the shape is weaker than needed in [3] for an the analysis of the  $\gamma$ -ray multiplicity encountered for fission of  $^{224}\text{Th}$ .
- However, it must be said that we have not yet striven for quantitative agreements. For instance, there is room for a more appropriate choice of the two parameters of collisional damping. In the present paper only their "standard choice" has been used, but as discussed in [9] these values are open for changes within a certain margin, and as demonstrated in [8], such modifications will not only change the values of the transport coefficients but also their variation with  $T$ . Furthermore, one should mention the influence of pairing, which still might be important at the smaller  $T$  value of 1 MeV, but which we have left out for the sake of simplicity. Moreover, the influence of angular momentum ought to be taken into account (see below). It should be said, of course, that the numbers extracted from comparisons with experiment are model dependent. Moreover, in simplified studies often Kramers' picture is applied, even in cases where the barrier is too low to guaranty that the flux across the barrier can be described by Kramers' solution of the Fokker-Planck equation. This problem can only be cured by performing genuinely dynamical studies along the lines reported in [26], [20], [30], [31], [32] but where all ingredients into macroscopic descriptions with Fokker-Planck or Langevin equations come from the same theory.
- Finally, we like to come back to angular momentum, once more, which influences fission dynamics in manyfold way. First of all, it changes the quasi-static energy through the centrifugal potential. Generally, this reduces the height of the barrier and thus restricts further the range of temperatures for which (3.4) is applicable. The centrifugal force will also modify the local stiffness and thus the coupling constant  $k$  through (2.8), which in turn effects the local response in various ways. However, even in zero frequency limit rotations will have sizable impact on the transport coefficients. This has been demonstrated in [33] for the case of friction. The reason for such a behavior is found in the fact that in the rotating frame the level structure may become very different from the one without rotations.

## Acknowledgments

The authors want to thank A.S. Jensen for valuable discussions and suggestions, as well as the Deutsche Forschungsgemeinschaft for financial support. Two of us (S.Y. and F.A.I.) like to thank the Physics Department of the TUM for the hospitality extended to them during their stay.



# References

- [1] D. Hilscher and H. Rossner, Ann. Phys. Fr. **17** (1992) 471
- [2] D. Hilscher, I.I. Gontchar and H. Rossner, Physics of Atomic Nuclei **57** (1994) 1187-1199
- [3] P. Paul and M. Thoennessen, Ann. Rev. Part. Nucl. Sci. **44** (1994) 65
- [4] J.Blocki, Y.Boneh, J.R.Nix, A.J.Sierk, W.J. Swiatecki, Ann. Phys. **113** (1978) 330
- [5] W.J. Swiatecki, Nucl. Phys. **A574** (1994) 233c
- [6] S. Yamaji, H. Hofmann and R. Samhammer, Nucl. Phys. **A475** (1988) 487
- [7] H. Hofmann, R. Samhammer and S. Yamaji, Phys. Lett. **B229** (1989) 309
- [8] H. Hofmann, F.A. Ivanyuk and S. Yamaji, Nucl. Phys. **A598** (1996) 187
- [9] H. Hofmann, submitted to Physics Reports
- [10] D. Kiderlen, H. Hofmann and F.A. Ivanyuk, Nucl.Phys. **A550** (1992) 473
- [11] P.J. Siemens and A.S. Jensen, "Elements of Nuclei: Many-Body Physics with the Strong Interaction", Addison and Wesley, 1987
- [12] H. Hofmann, Phys. Lett. **61B** (1976) 423
- [13] A. Bohr and B.R. Mottelson, Nuclear Structure, Vol.II (Benjamin,London,1957)
- [14] W. Brenig, "Statistical Theory of Heat, Nonequilibrium Phenomena", Springer, 1989, Berlin
- [15] H. Hofmann, S. Yamaji and A.S. Jensen, Phys. Lett. **B286** (1992) 1
- [16] F.A. Ivanyuk, H. Hofmann, V.V. Pashkevich and S. Yamaji, to be published
- [17] J. Maruhn and W. Greiner, Z.f.Phys. **251** (1972) 431
- [18] S. Yamaji and A. Iwamoto, Z.f.Phys. **A313** (1983) 161
- [19] D. Scharnweber, W. Greiner and U. Mosel, Nucl.Phys. **A164** (1971) 257
- [20] T. Wada, Y. Arimoto, M. Ohta, A. Abe and S. Yamaji, 2nd RIKEN-INFN Joint Int. Conf. on "Heavy Ion Collisions"(Wako), World Scientific, Singapore, (1995)
- [21] C. Guet, E. Strumberger and M. Brack, Phys.Lett. **B205** (1988) 427
- [22] H.J. Krappe, J.R. Nix and A. Sierk, Phys.Rev. **C20** (1979) 992
- [23] M. Bolsterli, E.O. Fiset, J.R. Nix and J.L. Norton, Phys. Rev. **C5** (1972) 1050
- [24] J.R. Nix and A. Sierk, Preprint LA-UR-86-698 (1986)
- [25] K.T.R. Davies, A.J. Sierk and J.R. Nix, Phys.Rev. **C13** (1976) 2385

- [26] P. Fröbrich and I.I. Gontchar, Nucl.Phys. **A563**, (1993) 326
- [27] S. Ayik and W. Nörenberg, Z. Phys. **A309** (1982) 121
- [28] H.A. Kramers, Physica 7 (1940) 284
- [29] H. Hofmann, G.-L. Ingold and M. Thoma, Phys. Lett.B 317 (1993) 489
- [30] E. Strumberger, K. Dietrich and K. Pomorski, Nucl. Phys. A529 (1991) 522
- [31] T. Wada, A. Abe and N. Carjan, Phys.Rev.Lett. **70** (1993) 3538
- [32] K. Pomorski, J. Bartel, J. Richert and K. Dietrich, submitted to Nucl. Phys. A
- [33] K. Pomorski and H. Hofmann, Phys.Lett. **B263** (1991) 164

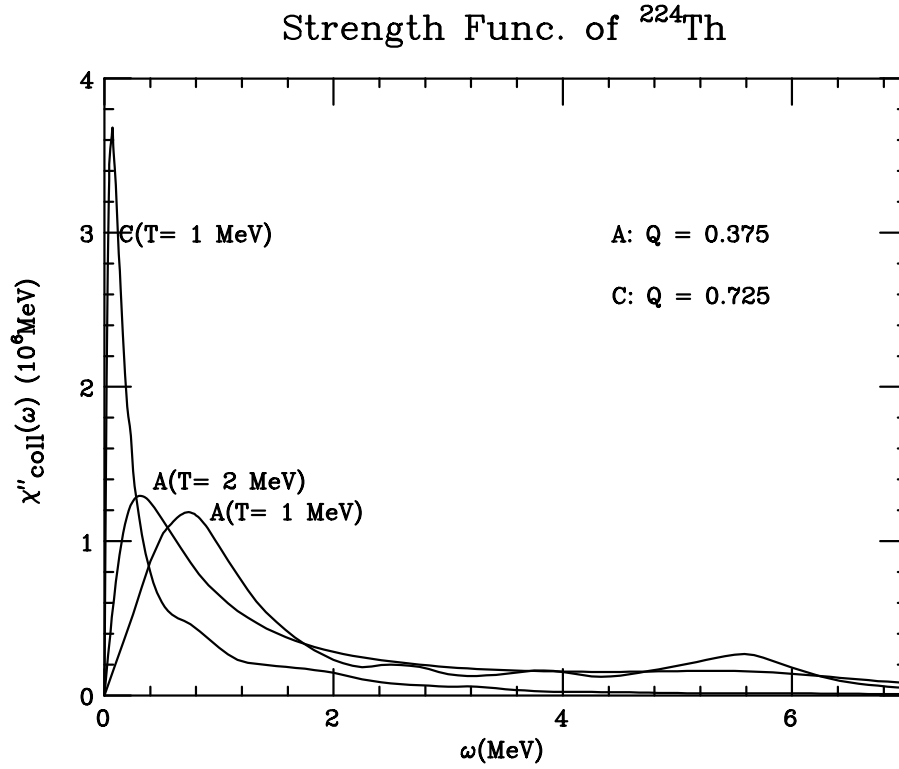


Figure 1: The imaginary part of the collective response function as a function of  $\omega$  at the points A and C for  $T = 1, 2, 3$  MeV

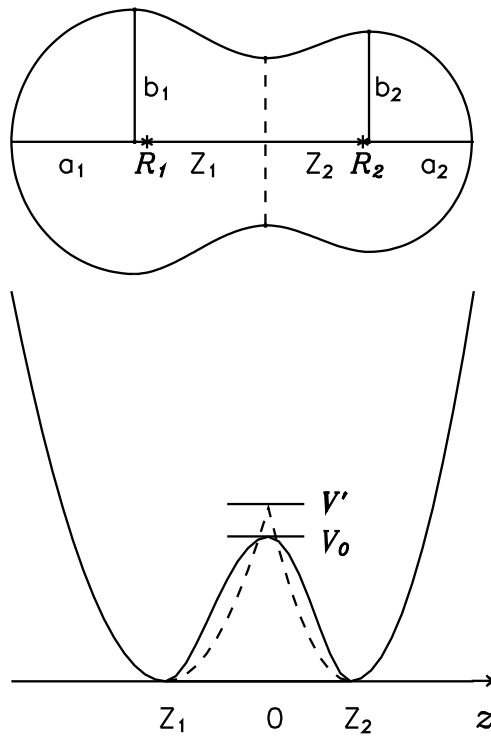


Figure 2: The potential along the  $z$ -axis and the nuclear shape.

Figure 3: The cold liquid-drop energy surface as functions of  $z_0$  and  $\delta$  for symmetric fission of  $^{224}\text{Th}$ . The long- and short-dashed curves show the minimal energy fission path and the configuration where two fragments start to separate, respectively. (*There exists no postscript file for this figure; the authors will be glad to send a hard copy upon request*)

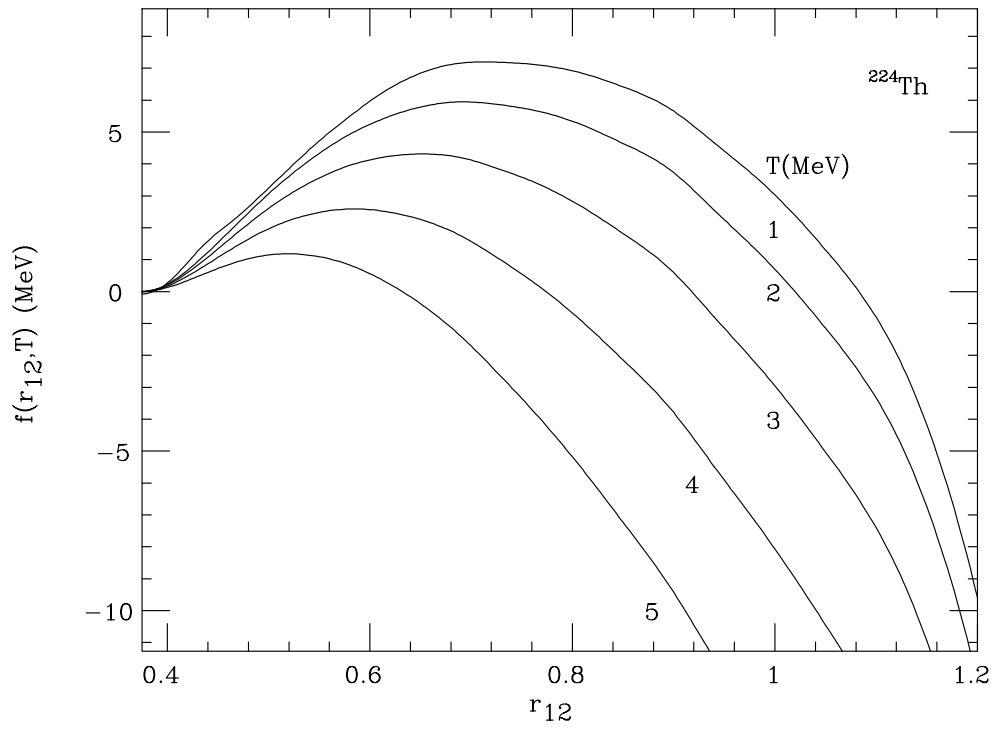


Figure 4: The free energy as a function of the shape variable  $r_{12}$  along the fission path for temperatures of 1, 2, 3, 4, and 5  $MeV$ .

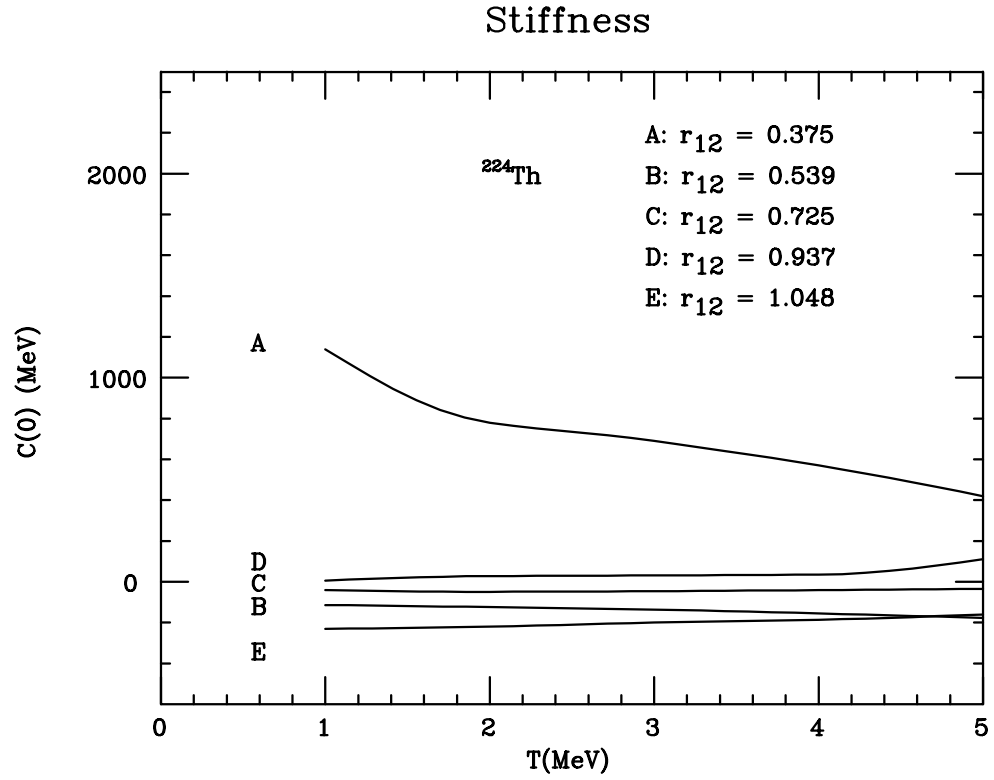


Figure 5: The local stiffness  $C(0)$  of the zero frequency limit as a function of  $T$  at the points A, C

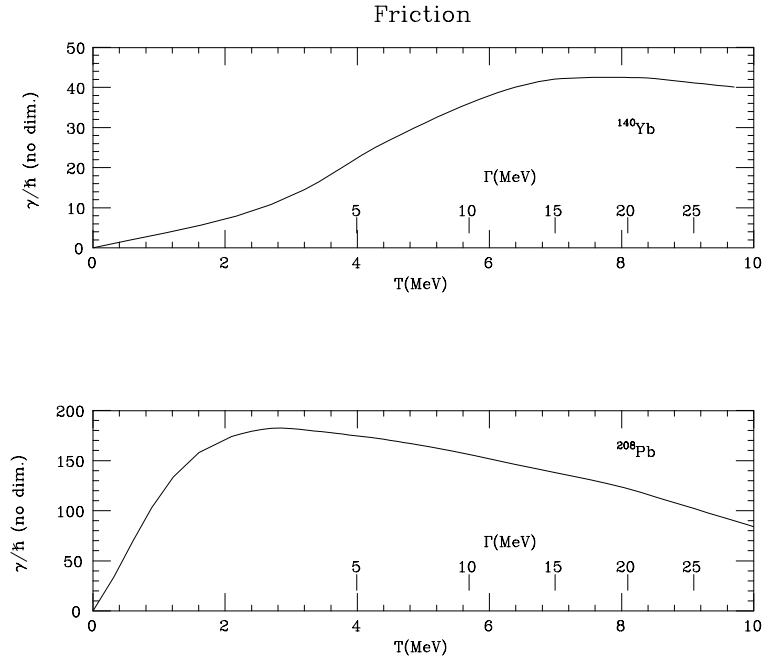


Figure 6: The temperature dependence of the friction coefficient Eq.(2.24) in the zero-frequency limit computed with the oscillator well. The shape variable  $Q$  corresponds to  $\delta$ . The computations are performed for the double magic nuclei  $^{140}\text{Yb}$  without spin-orbit coupling (upper) and  $^{208}\text{Pb}$  with spin-orbit coupling (lower)

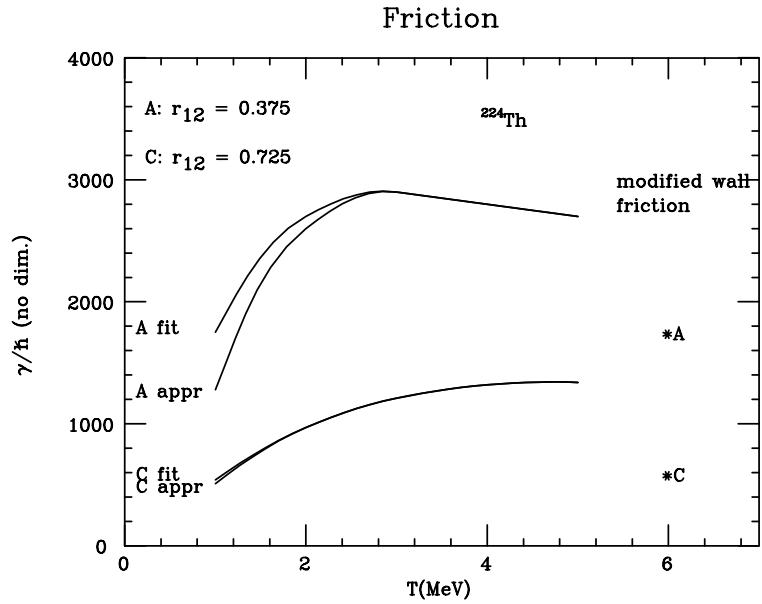


Figure 7: The friction coefficient  $\gamma$  obtained from the oscillator fit, shown as function of  $T$  at the points A-E

## Friction

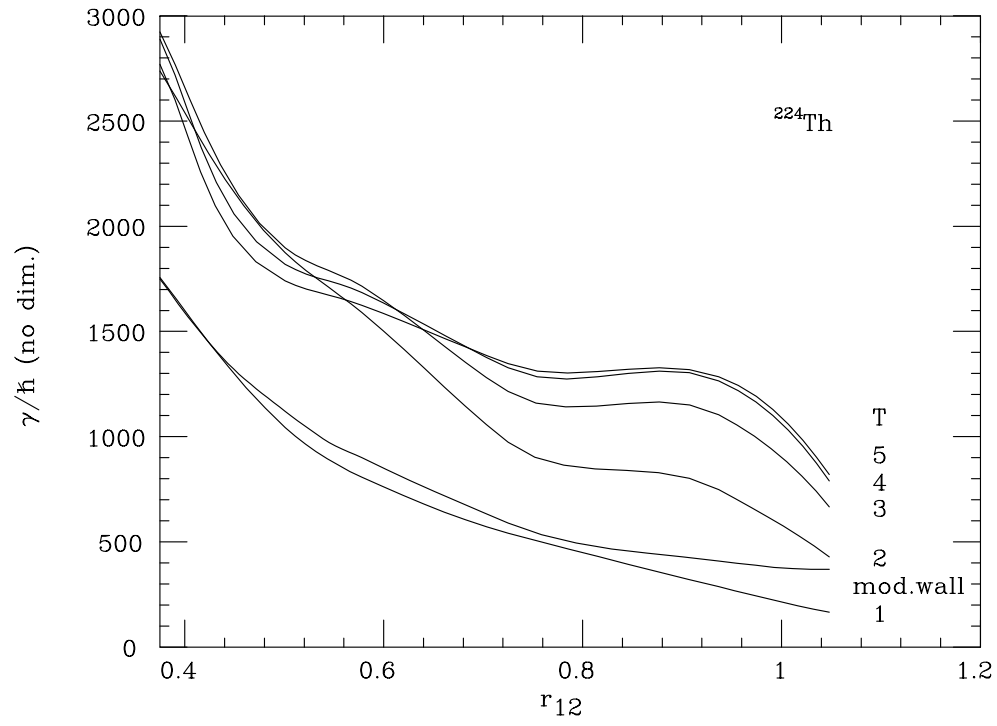


Figure 8: The friction coefficient  $\gamma$  as a function of  $r_{12}$  for  $T = 1-5 \text{ MeV}$

## Mass

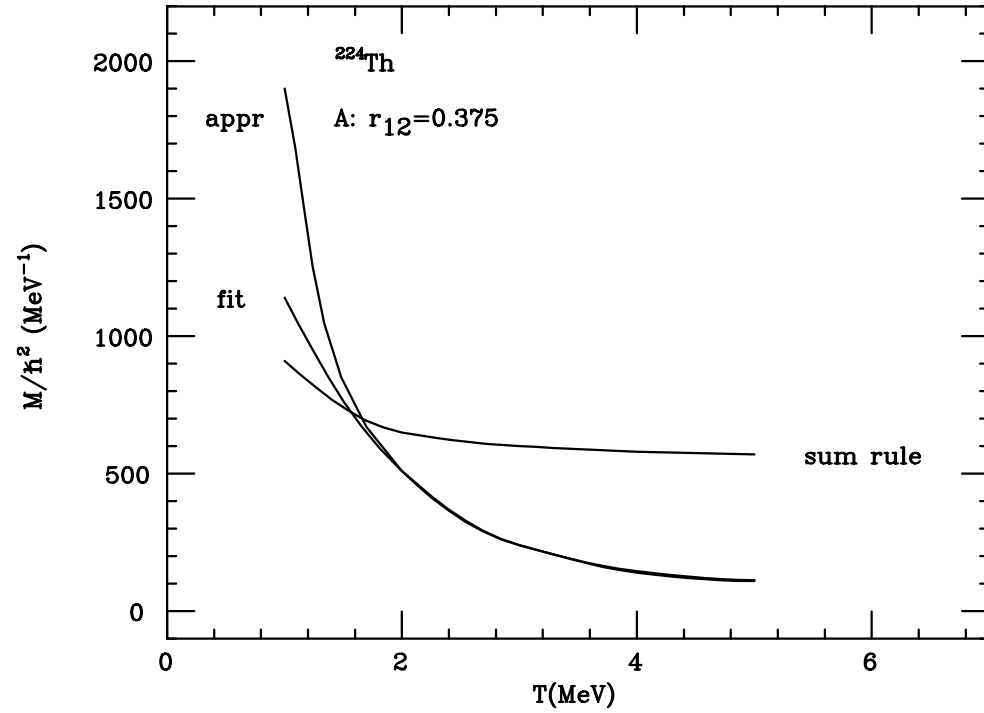


Figure 9: The inertia as a function of  $T$  at the point A, calculated by three different methods: (i) by the oscillator fit, (ii) by way of Eq.(2.18) and (iii) after obeying the sum rule (see text).

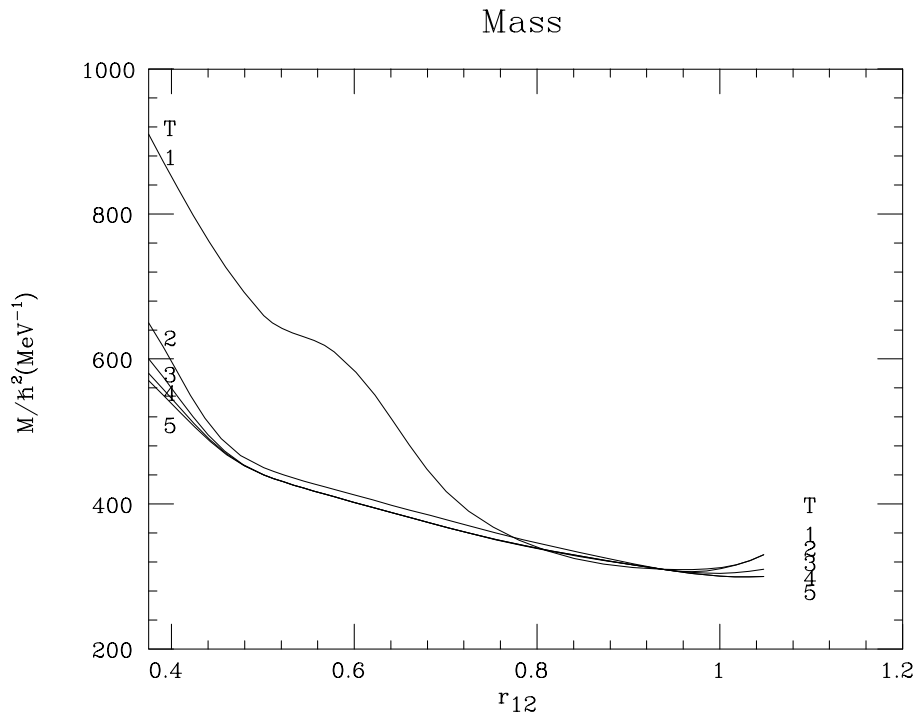


Figure 10: The inertia  $M$  satisfying the energy weighted sum rule as a function of  $r_{12}$  for  $T = 1-5$   $MeV$

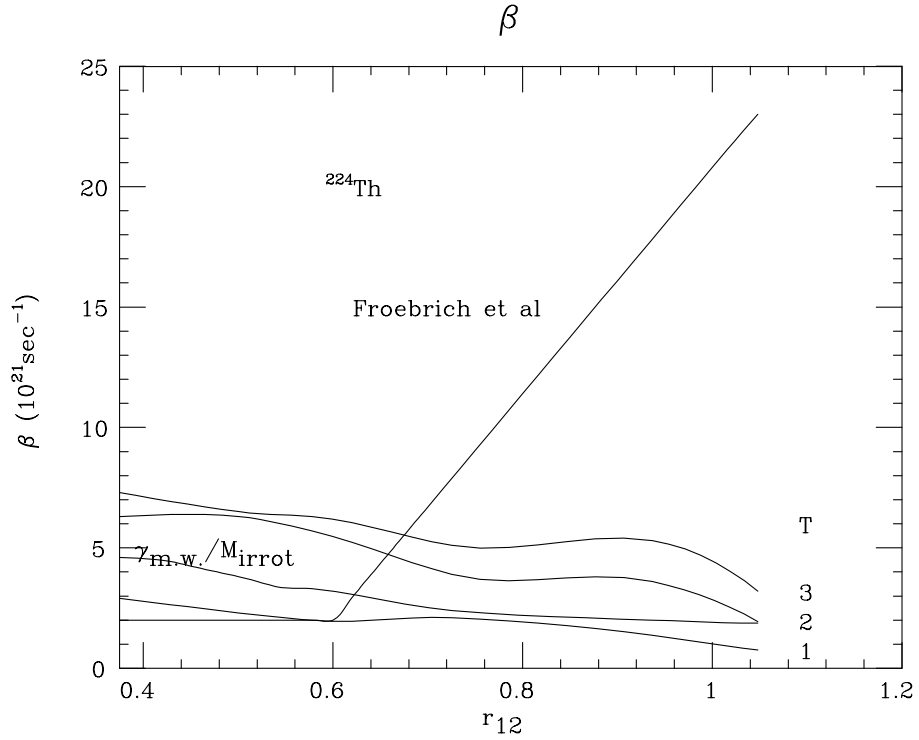


Figure 11:  $\beta = \gamma/M$  as function of  $r_{12}$  for  $T = 1-3$   $MeV$ ; for comparison we plot  $\beta = \gamma_{m.w.}/M_{irrot}$  and the empirical values from the analysis of Fröbrich et. al.